

Concept study of a lightweight high performance axial flux motor cooled with cryogenic hydrogen

André Baeten, Sabrina Barm, Markus Fackler, Neven Majic, Johannes Reitenberger, Timon Guenther, Christoph Lohr, Markus Sause, Anna Trauth, Richard Weihrich, Timo Koerner, Christian Oblinger

Angaben zur Veröffentlichung / Publication details:

Baeten, André, Sabrina Barm, Markus Fackler, Neven Majic, Johannes Reitenberger, Timon Guenther, Christoph Lohr, et al. 2023. "Concept study of a lightweight high performance axial flux motor cooled with cryogenic hydrogen." *SAMPE Journal* 59 (4): 59–69.
<https://doi.org/10.33599/nasampe/s.23.0059>.

Nutzungsbedingungen / Terms of use:

licgercopyright

Dieses Dokument wird unter folgenden Bedingungen zur Verfügung gestellt: / This document is made available under these conditions:

Deutsches Urheberrecht

Weitere Informationen finden Sie unter: / For more information see:

<https://www.uni-augsburg.de/de/organisation/bibliothek/publizieren-zitieren-archivieren/publiz/>



CONCEPT STUDY OF A LIGHTWEIGHT HIGH PERFORMANCE AXIAL FLUX MOTOR COOLED WITH CRYOGENIC HYDROGEN

André Baeten¹, Sabrina Barm¹, Markus Fackler¹, Neven Majic¹, Johannes Reitenberger¹

Timon Guenther², Christoph Lohr², Markus Sause², Anna Trauth², Richard Weihrich²

¹Augsburg University of Applied Sciences
Augsburg, Bavaria/Germany

²University of Augsburg
Augsburg, Bavaria/Germany

ABSTRACT

In this paper a concept study for a lightweight cryogenic hydrogen cooled axial flux motor is presented. The concept is based on a hybrid material design to fulfill the electro-magnetic, thermal, chemical, and mechanical requirements for a high-performance electrical drive train for Urban Air Mobility (UAM) applications. The concept study focuses on the virtual pre-design of the rotor stator combination and the cooling system using composites and ferromagnetic materials. FE and electro-magnetic performance simulation results based on trade studies will be presented as well as an outlook for the thermal and chemical material characterization the cooling system operated with cryogenic hydrogen.

Keywords: lightweight design, axial flux motor, hydrogen, cryogenic conditions, hybrid materials

Corresponding author: André Baeten

1. INTRODUCTION

1.1 Current state of the art and challenges in research

In the aerospace industry, electric motors have been identified as the major improvement in drive train technology concerning the reduction of pollutants and noise during a typical flight mission. Amongst the large number of concepts, two general electrical drive train architectures are of interest: battery-based systems and fuel cell-based systems. [1] In 2019, the first test aircraft HY4 of the German Aerospace Center (DLR) took off for its maiden flight. It is powered by fuel cells and batteries and can transport four people over several hundred kilometers. [2] Generally, the electric motors used in these aircraft are based on the electromagnetic interactions and the induced magnetic force effects between rotor and stator. In the present paper, the focus is on a hydrogen based electrical drive train using a hydrogen-cooled axial flux motor in contrast to conventional electrical motor architectures.

Copyright 2023. Used by the Society of the Advancement of Material and Process Engineering with permission.

SAMPE Conference Proceedings. Seattle, WA, April 17-20, 2023. Society for the Advancement of Material and Process Engineering – North America.

Compared to traditional radial flux electric motors, axial flux motors, especially “single stator – double rotor” topologies, are more effective in an electromagnetic sense. [3] Axial flux motors are generally differentiated into single stator single rotor (SSSR) such as shown in fig. 1, single stator double rotor (SSDR), double stator single rotor (DSSR) or multi-stator – multi-rotor (MSMR) architectures. Fig.2 shows different architectures.

These motors are already used in different industrial applications because of their compact structure and high torque capability. The major disadvantage of this type of electrical motor is the im-

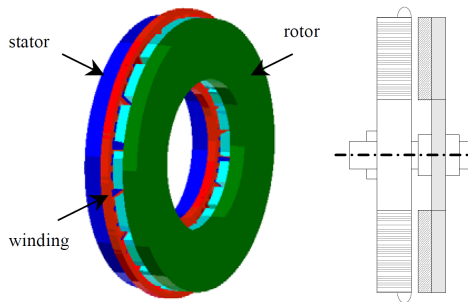


Figure. 1: Sketch of an axial flux motor with a single stator – rotor – configuration [14].

balanced axial force between stator and rotor, which may apply twist loads on the structure easily. In single stator – double rotor motors, the stator is located between two rotors and the main flux either travels axially through the stator or circular in the stator yoke while the torque is generated by radial direction windings. This structure is mainly preferred in applications where a lower cogging torque and torque ripple is required. [4] In double stator – single rotor axial flux motors, the rotor is located between two stators and the main flux flows either circular along the rotor disc or axial through the rotor disc. The double stator - single

rotor design can improve the effect of flux focusing and drive the flux to flow over dual air gaps and relatively decrease the leakage flux. [5] A multi-stator – multirotor motor can be constructed from either DSSR or SSDR configurations. The advantages and disadvantages of each construction are similar to their relevant preceding structures. This design has applications in ship propulsion, pumps and high-speed generators. [6]

High performance electrical motors can have an efficiency of 97% or higher, i. e. 3% of the elec-

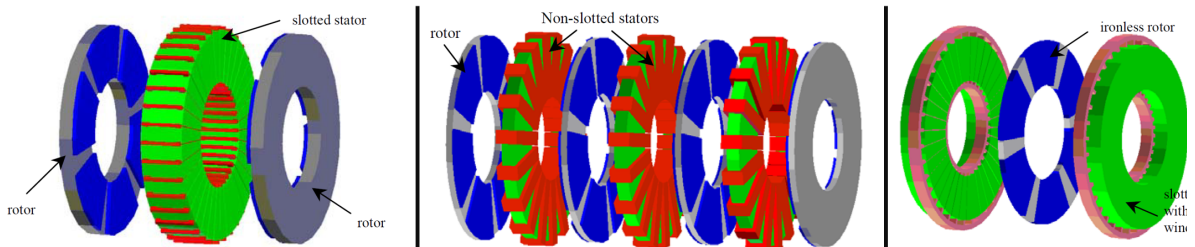


Figure.2: Examples of different stator-rotor-configurations for an axial flux motor [14].

trical energy is transferred into heat representing the electrical losses. Therefore, quick and efficient heat dissipation is mandatory in order to keep the point of operation in the high-power output regime. Consequently, a crucial factor in the design of high-performance axial flux motors is the cooling system. There are concepts where the cooling system is directly located in the motor compartment and the heat is dissipated via wire windings. In addition, external annular cooling systems are in use through which a specific cooling liquid circulates to dissipate the generated heat. There are also concepts with a direct stator cooling using an internal cooling pipe through which the liquid cooling medium is pumped. [7]

YASA for example has developed an axial flux motor with a comparatively low number of poles, manufactured with classic copper wires, with cooling outside the winding using conventional coolants. By using this method, the contact area between the cooling system and winding is small, thus

the motor only obtains a relatively low cooling efficiency. [8] Another manufacturer of such motors is the company MagniX, which develops propulsion systems for aviation based on the axial flux motor concept. These are classic motors, which are constructed conventionally, with a cooling that is as well carried out by means of a liquid, but in a small delta temperature range. [9] Thus, motors designed in this way can only be scaled to a limited extent due to the conventional design of the cooling system. Further, they cannot be operated in the overload range for an extended period, as due to the limited heat dissipation an overheating and thus a loss of power as well as the risk of a complete failure of the motor can occur. [10] However, according to the current state of the art, there are no concepts using hydrogen based hollow conductor cooling.

2. CONCEPT STUDY

2.1 Systemic approach of concept development

On its superordinate level, the systemic approach in this study follows the classic requirements driven process and V model of systems engineering such as described in [11]. The system of interest is the cooling system, integrated into an axial flux motor which again is integrated into an aircraft drivetrain as its meta system. An exemplary flight profile, representative for a (medium-range fixed-wing) Do228 aircraft, is considered in which the climb phase to an altitude of 30,000 [ft] is regarded. The total performance needs to achieve the respective climb rate, supposed to be met by two motors, amounts to 1200 [kW], respectively 600 [kW] per motor, for a duration of 720 [s]. The flight profile data plotted in fig. 3 is provided by the DLR.

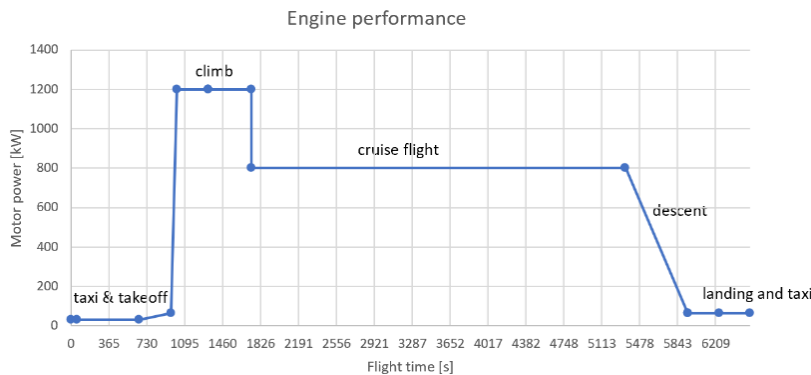


Figure 3: Exemplary flight profile and motor power requirements for a fixed-wing aircraft.

For the present study, a generic example for a single-rotor single-stator axial flux motor, like architectures described in [12], is assumed with an efficiency of 97%, resulting in 3% thermal loss power. Consequently, for a 600 [kW] electrical motor, the thermal losses amount to 18 [kW]. For further information about the efficiency of electrical motors, see

[15]. This contemplation does not include additional electric consumers and respectively produced waste heat in proximity to and thus influencing the motor. For the cooling system, the system analysis thus yields the functional requirement regarding the cooling performance of dissipating 18 [kW] over a time frame of 720 [s] to preserve integrity and functionality of the motor and its parts. [17]. In terms of non-functional requirements, the most significant requirement categories are manufacturability, lightweight requirements due to this cooling system being an aerospace application and hydrogen tightness requirements as a safety issue [20]. Fig. 4 shows the systemic approach, how functionalities and the ensuing physical architectures can be derived from the superordinate requirements.

The functional analysis is sketched in fig. 4 for a representative functional approach how the thermal energy can be transported out of the motor system. Generally, the mechanisms to transport thermal energy comprise radiation, conduction, and convection [13]. Here, an analytical estimate is conducted to evaluate the effectiveness of each mechanism. To provide a quick first estimate, the following abstractions and simplifications were made:

- Pressure is assumed to be constant throughout the tube system
- Hydrogen specific heat capacity is assumed to be constant at $c_p = 10840 \left[\frac{J}{kg \cdot K} \right]$ [13]
- Hydrogen temperature upon entry into cooling system is assumed to be $T_{hy,e} = 30$ [K]
- Pipe friction within an eventual medium transport tube is not considered in this estimate
- The axial flux motor is assumed to be installed in a closed compartment (adiabatic system), neglecting the influences of external air flow, surrounding air temperature and humidity
- Operating temperature for the axial flux motor is considered $T_{max} = 428$ [K] [17]; whereas operating temperatures are influenced by the respective winding insulation [17]

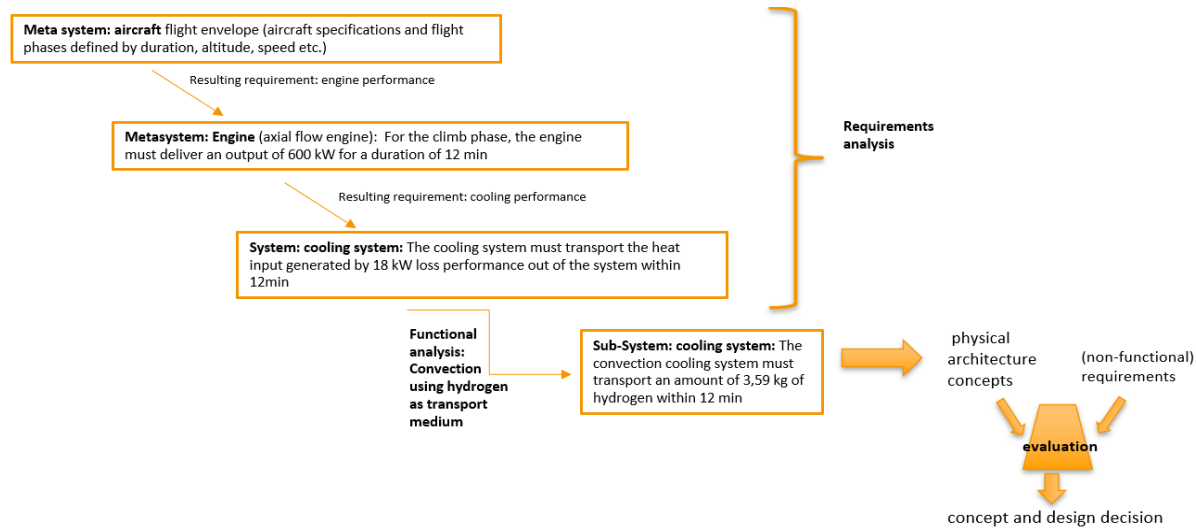


Figure 4: Systemic process of requirement-based derivation of concept decisions.

A Thermal Radiation

An estimate for dissipating the generated thermal energy via radiation can be made using the Stefan-Boltzmann-law [14] $\frac{\Delta Q}{\Delta t} = \epsilon * \sigma * A * T^4$; whereas $\sigma = 5,76 \cdot 10^{-8} \left[\frac{W}{m^2 \cdot K^4} \right]$ (Stefan-Boltzman constant) [14]. Furthermore, ϵ is approximated as $\epsilon=1$ and $A=338417,86$ [mm²]. The rate of heat dissipation thus yields 0,62 [kW], representing only 3,47% of the overall amount of 18 [kW], proving that radiation alone is not sufficient for heat dissipation.

B Thermal Conduction

The mechanical structure of the considered type of axial flux motor does not provide beneficial conditions for using conduction as heat transport mechanism. In general, metals show favourable capacities for thermal conduction [18]; Besides the motor topology, the choice of materials is a

promising parameter to fulfil the heat dissipation requirements. Consequently, the motor housing and fixations could be designed as metal structures. One metallic option respecting the lightweight restrictions could be an aluminium housing, such as described in [17]. However, the works of [17], studying a liquid cooling system in motor s with copper windings and aluminium housings, show that even using a TEFC (Totally Enclosed Fan Cooled) system and housing design configured to support cooling, the cooling performance using a liquid cooling is by far superior. In [18] the authors study thermal conduction, using copper bars in combination with liquid cooling, but their cooling concept does not rely on purely metallic conduction. Metallic conduction heat transfer alone is thus regarded as insufficient. Further, for lightweight reasons, essential parts of the stator – rotor configuration will be made of composite parts (CFRP) which show thermal conductivity inferior to metals, consequently the effectiveness of thermal conduction within that relatively small design space is not sufficient.

C Thermal Convection

The previously mentioned physically based estimates show that conduction and radiation do not allow for sufficient cooling performance to fulfil the heat dissipation requirements. Thermal convection, however, has proven enhanced capabilities for heat transport as described in [17].

In contrast to oil or specific cooling agents used for the studies in [17] and [18], the present study aims at using liquid hydrogen as cooling medium. Hydrogen is used in the drivetrain system as primary energy source, stored in liquid state. Upon entry into the cooling system, the hydrogen is assumed to be in gaseous state at a temperature of approximately 30 [K]. This assumption is based upon the transition from liquid state to gaseous state ensuing at temperatures above 20 K [28]. Further, during transport from the tank to the entry into the cooling system, friction and non-adiabatic effects occur increasing the temperature of the hydrogen. This factor is assumed to be of lower significance due to the pipe walls considered smooth [19] and will be considered in a quantified manner in ensuing studies. For the present example of 18 [kW] heat to be dissipated, the following numbers can be estimated.

Based on the loss power of 18 [kW], at $c_p = 10840 \left[\frac{J}{kg \cdot K} \right]$ as stated before and a temperature delta of $\Delta T = T_{op} - T_{hy,e} = 333 [K]$, an amount of 3,59 [kg] of cryogenic gaseous hydrogen is estimated to compensate the generated thermal energy of a temperature difference of 333 [K], which equals a flow rate of 0,005 [kg/s] for the duration of the climb phase.

Translating the functionality heat dissipation by convection using cryogenic gaseous hydrogen as transport medium into technically feasible solutions, different concepts have been elaborated. The basic parameters are choice of materials, cooling tube size and arrangement. Out of these possible technical solutions, three concepts, which do all fulfil the functional requirements, are compared in the following.

- Variant 1: Multiple tubes made of oxygen free copper;
- Variant 2: A singular tube made of oxygen free copper, and
- Variant 3: A singular tube made of STS 304 L (steel).

The tube cross-section is equal amongst all three concepts. In order to compare the three concepts in detail, first various non-functional requirements are assigned to the three concepts using a morphological box according to [21] and [22]. Second, the concepts are evaluated using a decision matrix according to [24] and shown in Table 1. Third, the specific material properties have been

evaluated separately referring to [23] and [20]. Chapter 2.3 deals with the cryogenic material characterization in detail. Table 2 shows the concept evaluation and identifies Variant 1 as optimal regarding the previously stated boundary conditions and assumptions.

comparison	1	less important	<i>property</i>	permeation properties	installation space usage	manufacturability	lightweight construction	service life duration
	2	equal importance						
	3	priority						
<i>property</i>								
permeation properties					1	1	1	1
installation space usage				3		2	1	1
manufacturability				3	2		2	1
lightweight construction				3	3	2		1
service life duration				3	3	3	3	
<i>sum</i>				12	9	8	7	4

Table 1: Property rating of the axial flux motor top level requirements.

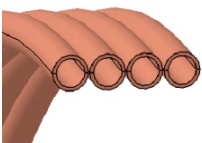
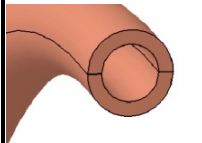
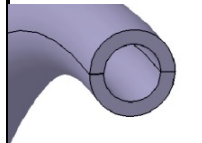
assessment 0 = unsatisfactory, 1 = acceptable in points (P) minimum, 2 = acceptable, 3 = good, 4 = very good		Variant 1		Variant 2		Variant 3	
assessment importance of criteria assigned to of percentage value from 0 to 1; sum evaluation amounts to 1							
<i>A</i>		OF Cu, thin multiple		OF Cu, thick singular		STS304L, thick singular	
	<i>P</i>	<i>P*A</i>		<i>P</i>	<i>P*A</i>	<i>P</i>	<i>P*A</i>
permeation properties	0,30	3	0,9	3	0,9	3	0,9
installation space usage	0,23	3	0,675	2	0,45	2	0,45
manufacturability	0,20	2	0,4	3	0,6	1	0,2
lightweight construction	0,18	1	0,175	1	0,175	1	0,175
service life duration	0,10	3	0,3	3	0,3	2	0,2
<i>Summ</i>	<i>1</i>	2,45		2,43		1,93	

Table 2: Concept assessment of the cryogenic hydrogen cooling system.

Further, safety requirements are significant for the subsystems and components as well as for the superordinate systems of the motor and drivetrain. However, regulations specific to hydrogen drivetrain certification for airworthiness are still in development. On the level of the cooling system and its components, hydrogen safety requirements concern primarily permeation properties, rated at highest importance in the property rating in Table 1. Airworthiness requirements are defined in [25] (EASA Directive Part 21.A „Airworthiness and Environmental Certification) and approval of aeronautic propulsion systems must be conducted in respect of EASA CS-E in its current amendment 6 from July 1st 2020 [26]. Subparts CS-E 140 – 170 treat requirements on motor, and motor subsystem and component testing.

2.2 Concept verification

[27] describes verification as “the confirmation, through the provision of objective evidence, that specified requirements have been fulfilled.” Objective evidence is usually an experimental assessment of a functional demonstrator of the system. Due to the extremely high costs of material characterization in cryogenic hydrogen atmosphere, physically based estimates, a thorough literature

survey and analogies are used to verify the presented concepts. For the Preliminary Design Review (PDR), however, testing will be done on Coupon level following the verification steps presented in table 3. On a systemic level, a technical demonstrator is supposed to be implemented and tested at a later point of the project to verify the functionality of the cooling system.

<i>property</i>	<i>verification method</i>	<i>verification description</i>
permeation properties	Exp+Test, Analogy	preparative literature research; permeation experiments on OF Cu and alternate materials such as STS304L
installation space usage	Simulation	Comparative installation space usage simulation using 3D models of each respective concept and the respective geometric arrangement variants
manufacturability	Analogy (market study)	Verifying manufacturability of concrete tube and cooling system geometries based upon state of the art manufacturing methods and industry availability
lightweight construction	Simulation	Comparative structural weight analysis using 3D models of each respective concept and the respective geometric arrangement variants
service life duration	Exp+Test, Simulation, Analogy	preparative literature research on fatigue strength, considering permeation properties related to material ageing. Conducting respective experiments on coupon level: mechanical fatigue and permeation tests on aged specimen

Table 3: Verification processes of the top-level system requirements.

2.3 Cryogenic material behavior and its influence on concept decisions

Storage systems and propulsion systems for liquid hydrogen are thermally and mechanically stressed in the range of cryogenic temperatures. In relation to the temperature range around room temperature – where different factors contribute to the heat transfer between gases, liquids, and solids –the material behavior is different at very low temperatures. On the one hand, the material parameters in the cryogenic range change in a non-linear manner, on the other hand, thermal radiation is also becoming significantly more important. As long as a cryogenic medium remains in the liquid state, the heat transfer with classic fluid mechanics and fluid-solid interaction applies. However, in the case of considerable heat inputs the energy inputs quickly lead to a phase transition liquid to gaseous which causes distinct discontinuous local effects. This must be considered in terms of fluid mechanics and the heat transfer. With most cryogenic liquids, the cryogenic gases allow a significantly higher heat dissipation than their liquid phase, so that this phase transition is often desirable in the operation of a technical structure [28]. For the design of aerospace-specific and safety-critical structures there are still deficits e.g., in the available failure criteria for composites, especially at cryogenic temperatures [29-31]. Therefore, experimental methods (see Chap.3 – Material Characterization) for detecting the progress of damage under cryogenic conditions are essential to refine design methods.

3. MATERIAL CHARACTERIZATION

Different specific testing methods for material characterization in cryogenic temperatures have been developed. State of the art is the use of cryogenic liquids and the introduction of the entire test device (immersion) into this liquid. However, this limits the test to the respective boiling temperature of the cryogenic liquid [32], [33], [36]. Recent concepts rely on cooling the test specimen

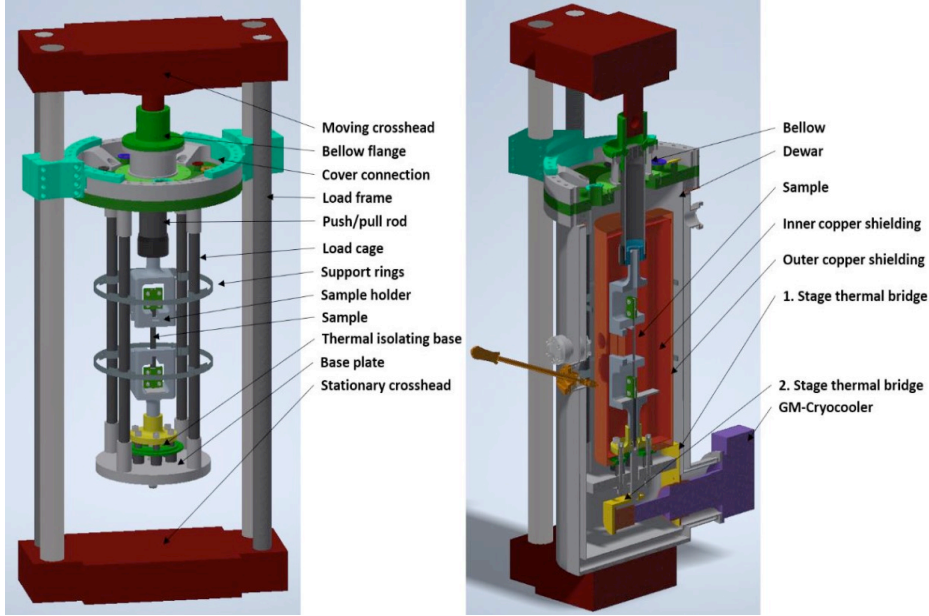


Figure 5: Detailed view of the load transmission path within the cryostat with tensile testing rig (left) and details of the thermal management of the cryostat (right) [37].

directly to the test temperature with cryogenic liquids or a cryogenic gas stream in combination with the test device in an insulated chamber. However, in this configuration it is almost impossible to determine characteristic values at a defined temperature since the test specimens heats up continuously without additional cooling. Likewise, it is not possible to reach very cold temperatures since the heat loss occurs within a very short time. To increase the functionality a temperature range, modern approaches use chillers to reach cryogenic temperatures in a closed cooling circuit. We recently developed a test setup based on a Gifford-McMahon cooler ([34], [35]) to overcome such limitations. A mechanical testing device is connected to the multi-stage Gifford-McMahon cooler via thermal bridges as shown in fig. 5. The Gifford-McMahon cryocooler pulls the first and second stage components to low temperatures with its cooling capacity (see fig. 5). The cooler/test setup is designed to operate at a load of 50 [kN] and allows for all conventional mechanical test setups, which fit into the inner testing space and can be equipped with AE Sensors and DIC setup [37]. Besides knowledge on structural material properties, several other material aspects need to be considered. The systemic approach has shown that in a fuel cell driven axial flux motor, hollow structures can be used to transfer the cryogenic hydrogen from the storage/ tank to the motor and through the motor's cooling system. There for long thin oxygen free copper tubes (OF-Cu) with diameters of around 3 to 10 mm are wound around the stator. [38] The constructive element of OF-Cu hollow structures allows heat management and cooling of the electric motor with the cryogenic hydrogen as well as its transport. Copper fulfills the demand of high electric and thermal conductivity ($5,26 \cdot 10^6 \text{ Sm}^{-1}$ [77 K] and $2430 \text{ W m}^{-1} \text{ K}^{-1}$ [20 K], [39]), low level of defects and stable performance under very low temperature of around 10 – 40 [K]. To minimize the corrosion and hydrogen embrittlement at very low temperatures and in contact with the highly corrosive and volatile hydrogen, OF-Cu is the material of choice. [39]

Due the liquid stored hydrogen, the thermodynamics and fluid mechanics play an important role in the system. A phase transition can take place when reaching temperatures higher than 20 [K] (-252,9 [°C]) at atmospheric pressure. Through modelling and simulation of the volume flow and heat transfer inside the OF-Cu hollow structure, the process can be described more detailed. Most critical is the process of Hydrogen corrosion as reaction of copper(I)-oxide with hydrogen which forms water or steam (> 100 [°C]). Dealing with temperatures way below 0 [°C], the water occurs in form of ice and can cause cracks or blasting of the copper tubes. The hydrogen corrosion is described in equation 1 [40]. To guarantee the stability of the copper structures, the amount of oxygen should not get higher than 400 ppm oxygen in the material. [46] Doping the copper with a low amount of phosphor (0.015 – 0.05 at.-%) can reduce the corrosion reaction due to the binding of oxygen with phosphor [40]. A decreased diffusion of oxygen into the metal and limiting the oxidation of copper to copper-oxide as a result.



The solubility of the small hydrogen molecules in copper in an equilibrium with 1 atm. hydrogen can be described by McLellan (1973) and Nakahara and Okinaka (1988) in equation 2. [41]

$$\ln \theta = - \frac{6.62 * 10^3}{T} - 4.48 \quad \text{equ. [2]}$$

T is the temperature in Kelvin, θ is 10^6 at. ppm. This means that at room temperature the amount of solved hydrogen is 40 at. ppm. At temperatures below 40 [K] the amount in OF-copper is even lower. More focus should be taken therefor on the supplied fuel flowing through the hollow structure without any oxygen to adsorb and cause hydrogen corrosion of the copper. Using long and thin copper hollow structures leads to a lower risk of defects in OF-copper from hydrogen embrittlement or corrosion. The oxygen-free copper is there for the state-of-art material to use.

4. FEM MODAL ANALYSIS AND CONCLUSIONS ON MATERIAL CHOICE

To make sure that an axial flux motor with a rotational frequency of 1591 [1/min] in flight application on the Do228 aircraft isn't driven in the range of the aircraft's eigenfrequencies, a finite element modal analysis (FEM) is conducted on a simplified CAD model [source: DLR]. The CAD model is based on geometrical approximations of the motor size of the Do228 aircraft. The main parts are the housing (blue), which is made of CFRP, a stator (grey) out of soft magnetic material, a copper coil (yellow) and a rotor (green) out of CFRP with integrated permanent magnets. To transfer the torque from the rotor to the shaft a connector (violet) out of stainless steel is used. The motor shaft is supported using two bearings (for simplification only represented as small red rings around the rotor shaft connection), see fig. 6. The CAD model is meshed in the FEM software Ansys mechanical. The tetrahedral mesh is created with 41506 nodes and 18149 elements (fig. 7). In the Do228 the motor needs to be fixated at the circumferentially arranged trapezoidal tabs with holes for mounting. In the simulation the tabs are therefore defined as fixed support. To define the

shaft support of the shaft, the rotor-shaft connection is defined as cylindrical support with rota-

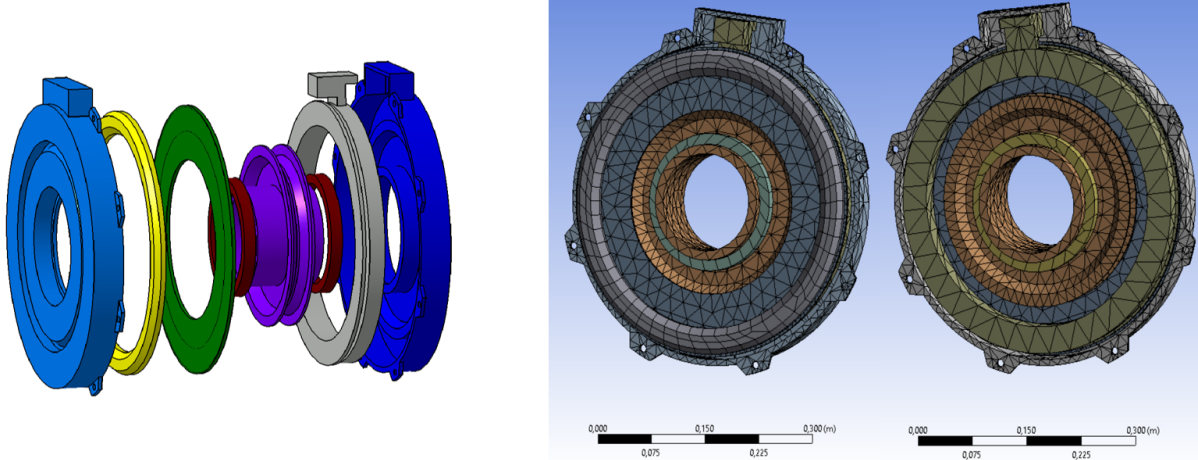


Figure 6: 3D-Views on the simplified CAD-model. Figure 7: Meshed CAD model in Ansys mechanical.

tional freedom around the shaft axis. Based on these boundary conditions a modal analysis is set up with the goal of determining six eigenfrequency modes. The results of the simulation are directly calculated; thus, no convergence analysis is applicable. The deformation of the housing for the eigenfrequency of 1473,2 [Hz] is shown in fig.8.

The six eigenfrequencies beginning at 1029 Hz at mode one up to 1473 [Hz] at mode six are plotted in fig. 9. Based on the low rotational speed of 1591 [rpm] (26,52 [Hz]), of the axial flux motor in

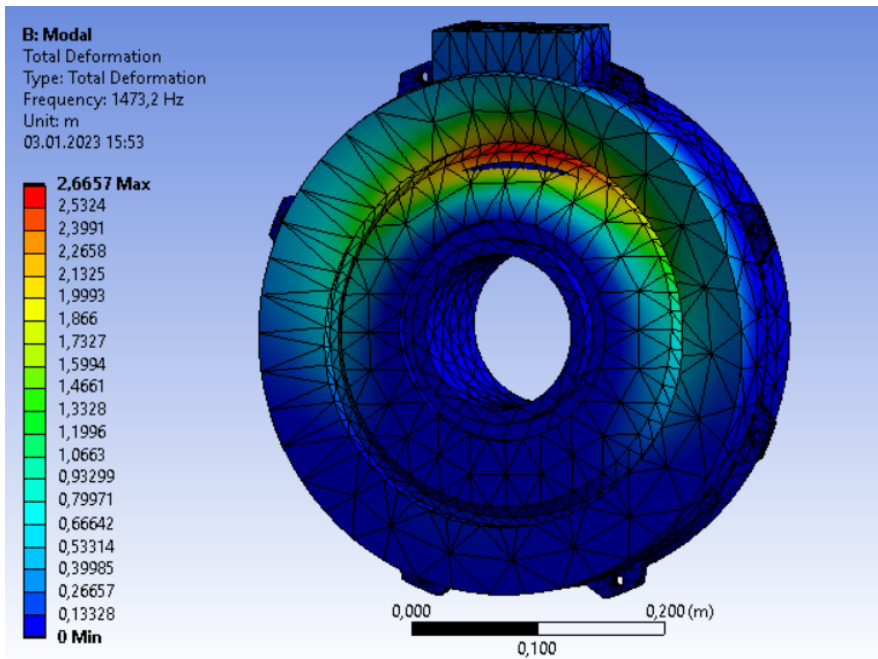


Figure 8: Deformation of the motor for the eigenfrequency 1473,2 [Hz].

results and experimental findings also showed that the first eigenfrequencies occur at about 1000 Hz [43].

the Do228 the mechanical motor frequency is much smaller than the lowest eigenfrequency of the motor at 1029 [Hz]. Note that this simulation does not include vibrations of neighboring aircraft components and electric or bearing induced vibrations.

Sunghyuk Park [43] performed a modal analysis to investigate the natural resonant frequencies of axial flux motors and a practical motor performance test as validation. Their simulation

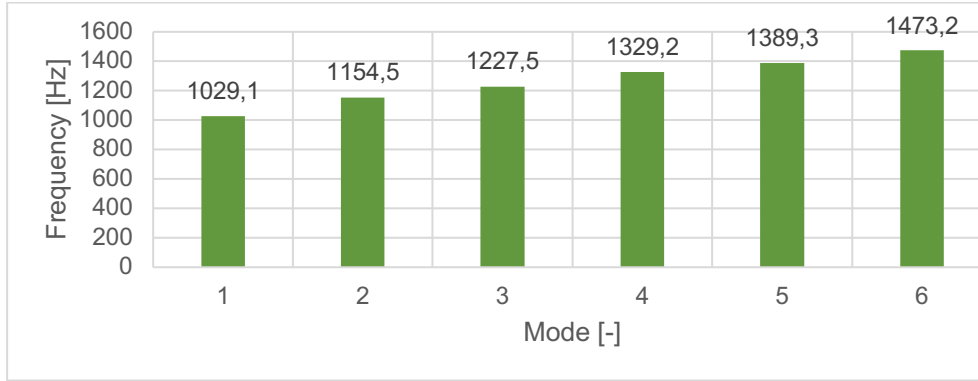


Figure 9: Calculated eigenfrequencies for the generic axial flux motor.

A noise-vibration-harshness analysis on axial flux motors of Kotter Philipp [42] shows critical eigenfrequencies at about 6000 rpm rotational speed of axial flux motors.

5. MANUFACTURING TECHNOLOGY

The integration of a cryogenic hydrogen-based cooling system into an axial flux motor requires a detailed look at the state-of-the art manufacturing technologies available today. Thereby, additive manufacturing provides the most flexible and integrative capabilities for the manufacturing of key components like the stator and the electromagnetic components made of specific metals. The numerous 3D printing processes available can be divided in powder or filament-based processes, respectively differed depending on the used materials. For the sub-area of metallic materials, powder bed systems have established themselves in industrial application. There are several different approaches like powder bed and inkjet head 3D printing (3DP), electron beam or selective laser melting (EBM/SLM), selective heat or laser sintering (SHS/SLS) or Direct metal laser sintering (DMLS). In contrast to this, there are processes with powder bound in a carrier medium as fused deposition modeling (FDM) where the process control and material volume needed is significantly reduced compared to powder bed process variations. In this context, Atomic Diffusion Additive Manufacturing (ADAM) is a particularly relevant process, as it allows for a quick material change for small scale production. Galati et. al [44] found however, that printed cubes from 17-4 PH Stainless steel with a layer thickness of 0,05 [mm] achieved a relative density of around 90%. It is known that the final sintering process has a significant impact on the final quality [44, 45]. Nevertheless, these systems are particularly well suited to study new tailor-made materials, as large amounts of powder do not have to be generated. Disadvantages can present themselves in the form of reduced material quality. Inferior mechanical properties in FDM manufactured parts have been found by [46]. In general, tensile strength of AM parts may be anisotropic and depend on build direction [47]. According to [47], AM processes are highly sensitive to parameter and material optimization and mistakes can result in “porosity, facilitating crack propagation and thus deteriorating mechanical properties”

Manufacturability and effective usage of the limited installation space have been stated as important non-functional properties and require great design freedom and the ability to manufacture challenging geometries. These issues are predestined to be addressed by additive manufacturing methods, thus eligible as manufacturing processes for notably the stator and the cooling system and respective components. This is especially true for geometrically integrative concepts combining several functionalities into one component.

As for the rotor, respectively the rotor disc having to exhibit significant deformation resistance, CFRP materials can provide optimal material properties in terms of stiffness and strength superior to metallic materials. The exact manufacturing process to choose will depend on the detailed manner of integration of the rotor magnets.

6. CONCLUSIONS

The present study deals with an axial flux motor cooled with cryogenic hydrogen for aircraft operations. Therefore, a generic axial flux motor is considered w.r.t. architecture and performance suitable for a fixed-wing aircraft of type Do228. For the specific power range of the motor, convection cooling using cryogenic hydrogen as cooling medium has been identified as the optimal heat transfer mechanism, compared to thermal radiation and thermal conduction. A technically feasible concept for the cooling system consisting of a multiple tube arrangement manufactured from OF-Cu (as discussed in Ch. 2.5), is presented, and evaluated against two further concept ideas. To fulfil EASA-conform safety requirements, cryogenic material behaviour is discussed based on the experience of the authors and a detailed literature survey. The concept evaluation results in a choice of materials and a motor topology that fulfils the technical and functional requirements of a 600 [kW] drivetrain suitable for the Do228. FEM-simulations carried out with the preliminary motor design show a good congruency with experimental results of other axial flux motors in terms of the first eigenfrequency and the mechanical loads. Finally, a short description of the manufacturing technology is presented with focus on the additive manufacturing technology.

The investigations in the mechanical, thermal and material domain show that a cooling system based on cryogenic hydrogen for axial flux motors for aircraft operations is feasible. The axial flux motor topology provides a good compromise of small cross section of the housing and high-power output due to a very good electromagnetic efficiency. The convective cooling using hydrogen as cooling agent requires only a small volume flux to maintain the motor power on over boost level for the entire climb phase. An application of this type of motor with hydrogen cooling system for Urban Air Mobility (UAM) seems promising as the available space for the drivetrain is limited and high over boost capabilities are required for start, hovering and manoeuvring.

7. OUTLOOK

The next step will be an extensive verification process to verify and detail the suggested concept as indicated in table 3, which will have to include studies in hydrogen phase transitions and their respective influence on heat dissipation. A detailed Design of Experiment (DoE) will be established including a series of material testing under cryogenic conditions, in combination with electromagnetic tests and safety tests concerning hydrogen permeation and inflammability. Material characterization under cryogenic conditions is discussed in Ch. 2.4 of this study. In further steps, the DoE will include experimental and simulative material characterization regarding mechanic properties under cryogenic conditions. The Coupon level tests will be the basis for component tests on the wiring level up to a full-scale functional demonstrator test series with the cooling system integrated into a generic axial flux motor running on a test bench.

Acknowledgements

This project is a collaboration between the University of Augsburg and the Augsburg University of Applied Sciences and is funded by the Bavarian Government (Bayerisches Staatsministerium

8. REFERENCES

1. M. Hepperle, "Electric Flight - Potential and Limitations", DLR, 2012
2. F. Oliviero, G. la Rocca, J. Sun, C. Varriale, "Optimal Control And Energy Management For Hybrid Aircraft", TU Delft, 2022
3. W. Geng, Y. Wang, J. Hou, J. Guo, Z. hang, "Comparative Study of Yokeless Stator Axial-Flux PM Machines having Fractional Slot Concentrated and Integral Slot Distributed Winding for Electric Vehicle Traction Applications", IEEE Transactions on Industrial Electronics, 2022
4. F. Caricchi, F. G. Capponi, F. Crescimbin, and L. Solero, "Experimental study on reducing cogging torque and no-load power loss in axial-flux permanent-magnet machines with slot-ted winding," IEEE Trans. Ind. Appl., 2004
5. F. Zhao, T.A. Lipo, B. Kwon, "A Novel Dual-Stator Axial-Flux Spoke-Type Permanent Magnet Vernier Machine for Direct-Drive Applications", IEEE Trans. Magn., 2014
6. F. Locment, E. Semail, and F. Piriou, "Design and study of a multiphase axial-flux machine," IEEE Trans. Magn., 2006
7. Dunn, MG. "Convective Heat Transfer and Aerodynamics in Axial Flow Turbines." *Turbo Expo: Power for Land, Sea, and Air*, 2001
8. J. Chang, Y. Fan, J. Wu, B. Zhu, "A yokeless and segmented armature axial flux machine with novel cooling system for in-wheel traction applications", IEEE Transactions on Industrial Electronics , 2021
9. H. Broch, "Direct Drive PMSM Characteristics for Retrofit in Regional Turboprops Using a "Design Space Approach", Norwegian University of Science and Technology, 2022
10. E. Gundabattini, A. Mystkowski, A. Idzkowski, R. Singh, D. Salomon, "Thermal Mapping of a High-Speed Electric Motor Used for Traction Applications and Analysis of Various Cooling Methods", Vellore Institute of Technology, 2021
11. I. Graessler, J. Hentze and T. Bruckmann, V-MODELS FOR INTERDISCIPLINARY SYSTEMS ENGINEERING. INTERNATIONAL DESIGN CONFERENCE - DESIGN 2018. DOI: 10.21278/idc.2018.0333
12. Aydin, M., S. Huang, T.A. Lipo, Axial Flux Permanent Magnet Disc Machines: A Review. Wisconsin Electric Machines&PowerElectronics Consortium, 2004.
13. J. Lienhard IV and J. Lienhard V, A heat transfer textbook. 5ft ed. Cambridge, Massachusetts: Phlogiston Press, 2020.
14. S. B. Giddings, Hawking radiation, the Stefan–Boltzmann law, and unitarization. Physics Letters B, Volume 754, Pages 39-42, ISSN 0370-2693, Elsevier, 2016. DOI:10.1016/j.physletb.2015.12.076.
15. S. Kahourzade, A. Mahmoudi, H. W. Ping and M. N. Uddin, A Comprehensive Review of Axial-Flux Permanent-Magnet Machines. *Canadian Journal of Electrical and Computer Engineering*, vol. 37, no. 1, pp. 19-33, 2014. DOI: 10.1109/CJECE.2014.2309322
16. G. Hunter, D. Makel, E. Jansa, G. Patterson, P. Cova, C. Liu, Q. Wu, W. Powers, A hydrogen leak detection system for aerospace and commercial applications. 31st Joint Propulsion Conference and Exhibit, 2012. DOI:10.2514/6.1995-2645
17. S. Jenwit, and C. Benyajati. "Liquid Cooled Induction Motor: Computational Design, Heat Transfer Analysis, Parametric Study, and Performance Testing." SAE International Journal

- of Alternative Powertrains, vol. 2, no. 1, 2013, pp. 1–6. JSTOR, <http://www.jstor.org/stable/26167714>. Accessed 5 Jan. 2023
18. J. Pyrhoenen, P. Lindh, M. Polikarpova, E. Kurvinen, V. Naumanen, Heat-transfer improvements in an axial-flux permanent-magnet synchronous machine. *Applied Thermal Engineering*, Volume 76, Pages 245-251, ISSN 1359-4311, 2015. DOI:10.1016/j.applthermaleng.2014.11.003.
 19. A. Demsis, S.V. Prabhu, A. Agrawal, Influence of wall conditions on friction factor for flow of gases under slip condition. *Experimental Thermal and Fluid Science*, Volume 34, Issue 8, Pages 1448-1455, ISSN 0894-1777, Elsevier, 2010. DOI:10.1016/j.expthermflusci.2010.07.008
 20. Kim, M.-S.; Lee, T.; Son, Y.; Park, J.; Kim, M.; Eun, H.; Park, J.-W.; Kim, Y. Metallic Material Evaluation of Liquid Hydrogen Storage Tank for Marine Application Using a Tensile Cryostat for 20 K and Electrochemical Cell. *Processes* 2022, 10, 2401. DOI:10.3390/pr10112401
 21. T. Ritchey, General morphological analysis (GMA). *Wicked problems—Social messes*. Berlin, Heidelberg, Springer, 2011.
 22. D. Rakov, Morphological methods of searching for new engineering solutions and their use in Industry 4.0. *Journal of Physics: Conference Series*, Volume 1679, Cybernetics and IT, 2020. DOI: 10.1088/1742-6596/1679/4/042083
 23. H. Horinouchi, M. Shinohara, T. Otsuka, K. Hashizume, T. Tanabe, Determination of hydrogen diffusion and permeation coefficients in pure copper at near room temperature by means of tritium tracer techniques, *Journal of Alloys and Compounds*, Volume 580, Supplement 1, Pages S73-S75, ISSN 0925-8388, 2013. DOI:10.1016/j.jallcom.2013.03.293
 24. Y. Bijan, J. Yu, J. Stracener, and T. Woods, Systems requirements engineering—State of the methodology. *Systems Engineering*, 16(3), 267-276, 2013. DOI:10.1002/sys.21227
 25. EASA Directive Part 21.A „Airworthiness and Environmental Certification
 26. EASA CS-E in its current amendment 6 from July 1st 2020
 27. V. Chapurlat, UPSL-SE: A model verification framework for Systems Engineering. *Computers in Industry*, Volume 64, Issue 5, Pages 581-597, ISSN 0166-3615, Elsevier, 2013. DOI:10.1016/j.compind.2013.03.002.
 28. C. Enss, S. Hunklinger, *Tieftemperaturphysik*. Springer-Verlag Berlin Heidelberg, pp. 465, 2000. DOI:10.1007/978-3-642-57265-4
 29. P. Soden, A. Kaddour, and M. Hinton, “Recommendations for designers and researchers resulting from the world-wide failure exercise,” *Composites Science and Technology*, vol. 64, no. 3-4, pp. 589–604, 2004, DOI: 10.1016/S0266-3538(03)00228-8.
 30. A. S. Kaddour, M. J. Hinton, and P. D. Soden, “A comparison of the predictive capabilities of current failure theories for composite laminates: additional contributions,” *Composites Science and Technology*, vol. 64, no. 3-4, pp. 449–476, 2004, DOI: 10.1016/S0266-3538(03)00226-4.
 31. A. S. Kaddour and M. J. Hinton, “Maturity of 3D failure criteria for fibre-reinforced composites: Comparison between theories and experiments: Part B of WWFE-II,” *Journal of Composite Materials*, vol. 47, no. 6-7, pp. 925–966, 2013, DOI:10.1177/0021998313478710.
 32. R. F. Nicholls-Lee, T. D. Bostock, and P. Watt, “Fully submerged composite cryogenic testing,” in 18th International conference on composite materials, 2011.

33. G. Geiss, "Einfluss von Tieftemperatur und Wasserstoff auf das Versagensverhalten von Glasfaser-Verbundwerkstoffen unter statischer und zyklischer Belastung," Universitaet Karlsruhe (TH), 2001.
34. R. Radebaugh, "Cryocoolers: the state of the art and recent developments," J. Phys. Condens. Matter, vol. 21, no. 16, p. 164219, Apr. 2009.
35. R. J. Huang, Q. Liu, L. F. Li, L. H. Gong, H. M. Liu, and D. Xu, "Cryogenic mechanical property testing system directly cooled by G-M cryocooler," 2014, pp. 81–85.
36. H. Haefele, A. Trauth and M.G.R. Sause, INVESTIGATION OF MODE I FRACTURE TOUGHNESS OF CARBON FIBER REINFORCED POLYMERS AT CRYOGENIC TEMPERATURES" – Proceedings of the 20th European Conference on Composite Materials, ECCM20. 26-30 June, 2022, Lausanne, Switzerland
37. L. Gabele, A. Trauth and M.G. R. Sause: "DEVELOPMENT OF A TEST RIG FOR THE TEMPERATURE-DEPENDENT DETERMINATION OF COMPOSITE MATERIAL PROPERTIES AT CRYOGENIC TEMPERATURES", Composites Meet Sustainability – Proceedings of the 20th European Conference on Composite Materials, ECCM20. 26-30 June, 2022, Lausanne, Switzerland
38. Oxygen-free Copper Cu-OF – Luvata Alloy OF-OK
39. EXPERIMENTAL TECHNIQUES FOR LOW-TEMPERATURE MEASUREMENTS: Cryostat Design, Material Properties, and Superconductor Critical-Current Testing, JACK W. EKIN, 2006
40. Estimation/Assessment of Oxygen content in copper by Metallographic method, Devdutt Singh, Vivek, Mittal , Subodh Rana, International Research Journal of Engineering and Technology (IRJET), 2018
41. Qiu, Y.; Yang, H.; Tong, L.; Wang, L. Research Progress of Cryogenic Materials for Storage and Transportation of Liquid Hydrogen. Metals 2021, 11, 1101. DOI:10.3390/met11071101
42. Kotter, Philipp; Morisco, David; Boesing, Matthias; Zirn, Oliver; Wegener, Konrad (2018): Noise-Vibration-Harshness-Modeling and Analysis of a Permanent-Magnetic Disc Rotor Axial-Flux Electric Motor. In: IEEE Trans. Magn. 54 (3), S. 1–4. DOI: 10.1109/TMAG.2017.2759244
43. Park, Sunghyuk; Kim, Wonho; Kim, Sung-Il (2014): A Numerical Prediction Model for Vibration and Noise of Axial Flux Motors. In: IEEE Trans. Ind. Electron. 61 (10), S. 5757–5762. DOI: 10.1109/TIE.2014.2300034
44. Galati M, Minetola P. Analysis of Density, Roughness, and Accuracy of the Atomic Diffusion Additive Manufacturing (ADAM) Process for Metal Parts. Materials (Basel). 2019 Dec 9;12(24):4122. DOI:10.3390/ma12244122. PMID: 31835380; PMCID: PMC6947362.
45. Henry, T.C., Morales, M.A., Cole, D.P. et al. Mechanical behavior of 17-4 PH stainless steel processed by atomic diffusion additive manufacturing. Int J Adv Manuf Technol 114, 2103–2114 (2021).
46. S. Singh, S. Ramakrishna, R. Singh, Material issues in additive manufacturing: A review. Journal of Manufacturing Processes, Volume 25, Pages 185-200, ISSN 1526-6125, 2017, DOI:10.1016/j.jmapro.2016.11.006.
47. D. Herzog, V. Seyda, E. Wycisk, C. Emmelmann, Additive manufacturing of metals. Acta Materialia, Volume 117, Pages 371-392, ISSN 1359-6454, 2016. DOI:10.1016/j.actamat.2016.07.019.